Structural Engineering and Mechanics, Vol. 26, No. 6 (2007) 687-707
DOI: http://dx.doi.org/10.12989/sem.2007.26.6.687

Generation of critical and compatible seismic ground acceleration time histories for high-tech facilities

X. J. Hong† and Y. L. Xu‡

Department of Civil and Structural Engineering, The Hong Kong Polytechnic University, Kowloon, Hong Kong, China

(Received February 3, 2006, Accepted February 21, 2007)

Abstract. High-tech facilities engaged in the production of semiconductors and optical microscopes are extremely expensive, which may require time-domain analysis for seismic resistant design in consideration of the most critical directions of seismic ground motions. This paper presents a framework for generating three-dimensional critical seismic ground acceleration time histories compatible with the response spectra specified in seismic design codes. The most critical directions of seismic ground motions associated with the maximum response of a high-tech facility are first identified. A new numerical method is then proposed to derive the power spectrum density functions of ground accelerations which are compatible with the response spectra specified in seismic design codes in critical directions. The ground acceleration time histories for the high-tech facility along the structural axes are generated by applying the spectral representation method to the power spectrum density function matrix and then multiplied by envelope functions to consider nonstationarity of ground motions. The proposed framework is finally applied to a typical three-story high-tech facility, and the numerical results demonstrate the feasibility of the proposed approach.

Keywords: high-tech facility; critical seismic directions; acceleration time history generation; response spectrum compatibility.

1. Introduction

The research on the generation of earthquake ground acceleration time histories has been extensively studied in the last three decades. The generation approaches can be classified into two categories in general. One is the seismology method, and the other is the engineering method. Seismology method involves seismic source model, elastic rebound theory, and elastic wave theory. Joshi and Midorikawa (2004) proposed a simplified seismology method for simulating strong ground motion for a representation of a finite earthquake source buried in a layered earth based on the empirical Green function. Engineering method mainly relies on measured data or definite acceleration spectra. Crempien-Laborie and Orosco (2000) proposed an engineering method to simulate artificial acceleration records based on the theory of non-stationary random processes with evolutionary acceleration spectra. The ARMA model is also employed (Olafsson *et al.* 2001) for simulating ground motion in Iceland using the measured data. Taskin and Hasgur (2006) simulated

† Research Associate, E-mail: cehongxj@polyu.edu.hk
‡ Chair Professor, Corresponding author, E-mail: ceylxu@polyu.edu.hk

strong ground motions from the Gaussian white-noise random process with Kanai-Tajimi filter. However, the seismic ground acceleration time histories generated by the aforementioned engineering methods are often in one direction only and are not compatible with response spectra provided by seismic design codes for building structures.

High-tech facilities engaged in the production of semiconductors and optical microscopes are extremely expensive. When high-tech facilities are located in seismic regions, the safety of both building and high-tech equipment during an earthquake becomes a critical concern, and the seismic resistant design of high-tech facilities faces a number of challenging issues. For instance, seismic ground motion can act along any horizontal direction, and the maximum structural and equipment response associated with the most critical directions of seismic ground motions should be examined. Moreover, not only horizontal accelerations but also vertical acceleration will affect the safety of high-tech equipment, and accordingly three-dimensional seismic analysis should be carried out. Since high-tech equipment sitting on a building floor is very heavy and may not be uniformly distributed over the building floor, possible torsion vibration of the building during an earthquake may occur even though the building itself is symmetric. To reduce seismic vibration of both building and high-tech equipment, vibration control technique with linear and nonlinear dampers may be implemented into a high-tech facility. Therefore, it requires the three-dimensional seismic analysis of a high degree of accuracy for a high-tech facility in the time domain with respect to the most critical directions of seismic ground motion. Furthermore, because most seismic analysis of a building is based on the response spectra specified in seismic design codes (e.g., Li and Li (2005)), how to generate three-dimensional critical seismic ground acceleration time histories compatible with the response spectra specified in seismic design codes becomes a primary issue prior to seismic analysis and design of a high-tech facility.

Therefore, instead of using the existing ground acceleration spectra such as Clough-Penzien spectrum or Kanai-Tajimi spectrum in the previous studies, this paper presents a framework for generating three dimensional critical seismic ground acceleration time histories compatible with the response spectra specified in seismic design codes. The most critical directions of seismic ground motions associated with the maximum structural and equipment response of a facility are alwalys identified based on the response spectrum method (e.g., Lopez and Torres 1997, Menum and Der Kiureghian 1998) for the general case of three motion components. A new numerical method is then proposed to derive the power spectrum density functions of ground accelerations which are compatible with the response spectra specified in seismic design codes in critical directions. The ground acceleration time histories are generated by applying the spectral representation method to the power spectrum density function matrix and then multiplied by envelope functions to consider nonstationarity of ground motions. The proposed framework is finally applied to a three-story reinforced-concrete high-tech building to demonstrate its effectiveness.

2. Maximum response and critical direction

The maximum structural response associated with the most critical directions of seismic ground motions has been examined by Lopez and Torres (1997), Menun and Der Kiureghian (1998) among others. Since this study concerns the seismic resistant design of high-tech facilities using response spectra specified in seismic design codes, the response spectrum method proposed by Lopez and Torres (1997) is adopted and reviewed in this section for the sake of completion.

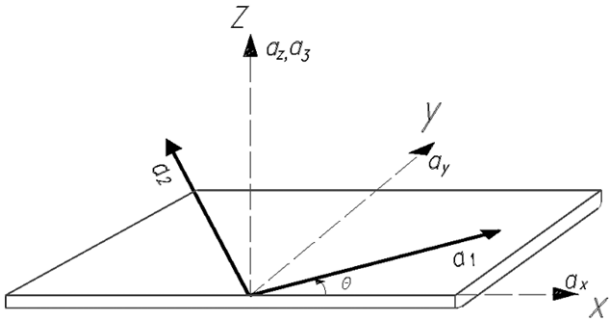

Fig. 1 Principal directions and structure axes

Fig. 1 illustrates the situation of a structure subject to the simultaneous action of two orthogonal horizontal ground accelerations $a_1(t)$ and $a_2(t)$ in directions 1 and 2, respectively, and one vertical ground acceleration $a_3(t)$ in direction 3. Directions 1, 2 and 3 are the principal directions of the earthquake with direction 1 toward the epicenter. The components of ground accelerations $a_1(t)$, $a_2(t)$ and $a_3(t)$ are thus statistically independent with the maximum, intermediate and minimum intensity respectively. In Fig. 1, X, Y and Z are the three reference axes of the structure, in which the Z-axis is the same as the principal direction 3 and the principal direction 1 is at an incidence angle θ with the X-axis. Clearly, the ground acceleration components in the structural coordinate are related to those in the principal coordinate as follows

$$\begin{Bmatrix} a_x \\ a_y \\ a_z \end{Bmatrix} = \mathbf{R} \begin{Bmatrix} a_1 \\ a_2 \\ a_3 \end{Bmatrix} = \begin{bmatrix} \cos\theta & -\sin\theta & 0 \\ \sin\theta & \cos\theta & 0 \\ 0 & 0 & 1 \end{bmatrix} \begin{Bmatrix} a_1 \\ a_2 \\ a_3 \end{Bmatrix} \tag{1}$$

where a_x, a_y, and a_z are the ground acceleration components along the X-, Y- and Z-axes of the structure; and $\mathbf{R}$ is the transformation matrix. Let us consider a liner elastic structural system of n-degrees of freedom. If r^1, r^2, and r^3 denote the contributions to a response quantity of the structure respectively from the principal ground accelerations $a_1(t)$, $a_2(t)$ and $a_3(t)$, they can be determined based on the response spectrum method proposed by Lopez and Torres (1997) as follows

$$(r^1)^2 = \sum_{i=1}^{n}\sum_{j=1}^{n} c_{ij} r_i^1 r_j^1 = \sum_{i=1}^{n}\sum_{j=1}^{n} c_{ij} r_i^{1x} r_j^{1x} \cos^2\theta + \sum_{i=1}^{n}\sum_{j=1}^{n} c_{ij} r_i^{1y} r_j^{1y} \sin^2\theta + 2\sum_{i=1}^{n}\sum_{j=1}^{n} c_{ij} r_i^{1x} r_j^{1y} \sin\theta\cos\theta \tag{2}$$

$$(r^2)^2 = \sum_{i=1}^{n}\sum_{j=1}^{n} c_{ij} r_i^2 r_j^2 = \sum_{i=1}^{n}\sum_{j=1}^{n} c_{ij} r_i^{2y} r_j^{2y} \cos^2\theta + \sum_{i=1}^{n}\sum_{j=1}^{n} c_{ij} r_i^{2x} r_j^{2x} \sin^2\theta - 2\sum_{i=1}^{n}\sum_{j=1}^{n} c_{ij} r_i^{2x} r_j^{2y} \sin\theta\cos\theta \tag{3}$$

$$(r^3)^2 = \sum_{i=1}^{n}\sum_{j=1}^{n} c_{ij} r_i^3 r_j^3 \tag{4}$$

where c_{ij} denotes the correlation coefficient between the responses in modes i and j, which is identical to that used in the complete quadratic combination (CQC) rule; r_i^1, r_i^2 and r_i^3 are the contributions to the response quantity in the ith mode of vibration of the structure respectively from the principal ground accelerations $a_1(t)$, $a_2(t)$ and $a_3(t)$; r_i^{1x} and r_i^{1y} are the contributions to the

response quantity in the ith mode of vibration when the principal ground acceleration $a_1(t)$ acts along the X- and Y-axis of the structure respectively; r_i^{2x} and r_i^{2y} are the contributions to the response quantity in the ith mode of vibration when the principal ground acceleration $a_2(t)$ acts along the X- and Y-axis of the structure respectively. Since the three principal grounds accelerations are statistically independent, the total response of the structure is given by

$$r = [(r^1)^2 + (r^2)^2 + (r^3)^2]^{1/2} \tag{5}$$

Clearly, the total response r is the function of the seismic incidence angle θ. It is not difficult to derive the critical angle by solving equation $\partial r/\partial\theta = 0$. The critical angle that renders the maximal response of the structure is given by

$$\theta_c = \frac{1}{2}\tan^{-1}\left\{\frac{2\sum_i^n\sum_j^n c_{ij}[r_i^{2y}r_j^{2x} - r_i^{1x}r_j^{1y}]}{(r^{1y})^2 + (r^{2x})^2 - (r^{1x})^2 - (r^{2y})^2}\right\} \tag{6}$$

in which

$$r^{1x} = \left[\sum_{i=1}^n\sum_{j=1}^n c_{ij}r_i^{1x}r_j^{1x}\right]^{1/2}, \qquad r^{1y} = \left[\sum_{i=1}^n\sum_{j=1}^n c_{ij}r_i^{1y}r_j^{1y}\right]^{1/2}$$
$$r^{2x} = \left[\sum_{i=1}^n\sum_{j=1}^n c_{ij}r_i^{2x}r_j^{2x}\right]^{1/2}, \qquad r^{2y} = \left[\sum_{i=1}^n\sum_{j=1}^n c_{ij}r_i^{2y}r_j^{2y}\right]^{1/2} \tag{7}$$

Eq. (6) has two roots separated by 90° and corresponding to those values of θ that give the maximum and minimum values of the response r in Eq. (5). It is noted that the critical angles do not depend on the vertical response r^3 and hence do not depend on the vertical ground acceleration.

3. Power spectrum density functions of ground acceleration

It is well known that three principal ground accelerations $a_1(t)$, $a_2(t)$ and $a_3(t)$ can be simulated in the time domain provided that the corresponding power spectrum density functions are available. It is also well known that the standard seismic resistant design of a high-tech building is based on the response spectra specified in seismic design codes. Therefore, it is necessary to obtain the power spectrum density functions of ground accelerations from given acceleration response spectra. Several formulations have been proposed by different investigators to obtain the power spectrum density function compatible with the given response spectrum (Kaul 1978, Gupta and Trunific 1998). Many of these are based on some approximate statistical distribution of the maximum of a random function of time and some approximate treatment for the transient nature of seismic response. Some of these concern the conversion of ground displacement other than ground acceleration. In the present study, the problem in obtaining the power spectrum density function of ground acceleration compatible with the acceleration response spectrum is discussed analytically. A new numerical method is then proposed to tackle the problem.

3.1 Discussion

Let us assume that the ground acceleration is a stationary stochastic process and the single-degree-of-freedom (SDOF) system is linear and elastic. According to random vibration theory, the peak absolute acceleration response of the SDOF system subject to ground acceleration can then be given by

$$R(\omega_c, \xi_c) = r_P[\int_0^\infty S_E(\omega)|H(\omega_c, \xi_c, \omega)|^2 d\omega]^{1/2} = r_p \sigma(\omega_c, \xi_c) \tag{8}$$

where R is the peak absolute acceleration response which is equivalent to the acceleration response spectrum; r_p is the response peak factor; $S_E(\omega)$ is the one-side ground acceleration spectrum; $H(\omega_c, \xi_c, \omega)$ is the absolute acceleration response transfer function; and $\sigma(\omega_c, \xi_c)$ is the standard deviation of absolute acceleration response. The response peak factor can be given by

$$r_p = \sqrt{2\log(vT)} + \frac{0.577}{\sqrt{2\log(vT)}} \tag{9}$$

where v is often conservatively taken as the natural frequency in Hz; and T is the time interval over which the peak acceleration response occurs. It is noted that Eq. (9) is not recommended for v when its value is zero or infinite. The absolute acceleration response transfer function can be given by

$$|H(\omega_c, \xi_c, \omega)|^2 = \frac{1 + 4\xi_c^2 \dfrac{\omega^2}{\omega_c^2}}{\left(1 - \left(\dfrac{\omega}{\omega_c}\right)^2\right)^2 + 4\xi_c^2 \dfrac{\omega^2}{\omega_c^2}} = \frac{\omega_c^4 + 4\xi_c^2 \omega_c^2 \omega^2}{(\omega_c^2 - \omega^2)^2 + 4\xi_c^2 \omega_c^2 \omega^2} \tag{10}$$

where φ_c is the damping ratio of the system; ϖ_c is the natural circular frequency of the system. Let us consider the variance of the absolute acceleration response in Eq. (8) in terms of the double-side ground acceleration spectrum $S_e(\omega)$.

$$\sigma^2(\omega_c, \xi_c) = \int_{-\infty}^{+\infty} S_e(\omega)|H(\omega_c, \xi_c, \omega)|^2 d\omega \tag{11}$$

Suppose that the integrand in Eq. (11) is analytical in the half plane Im $\omega > 0$ and continuous in the half plane Im $\omega \geq 0$ except at the isolated singular points $\omega_1, \omega_2, \ldots, \omega_m$ and it satisfies the condition $\lim_{\omega \to \infty} \omega S_e(\omega)|H(\omega_c, \xi_c, \omega)|^2 = 0$ in the half plane Im $\omega \geq 0$. Then, according to the residue theorem, one can find the variance of the absolute acceleration response as follows.

$$\sigma^2(\omega_c, \xi_c) = 2\pi i \sum_{k=1}^{m} res(S_e(\omega)|H(\omega_c, \xi_c, \omega)|^2, \omega_k) = \frac{\pi \omega_c}{2\xi_c}(1 + 4\xi_c^2) S_e(\omega_c) \tag{12}$$

The double-side ground acceleration spectrum is then given by

$$S_e(\omega_c) = \frac{2\xi_c}{\pi|\omega_c|(1 + 4\xi_c^2)} \sigma^2(|\omega_c|, \xi_c) \tag{13}$$

An equivalent ground acceleration spectrum similar to Eq. (13) was proposed by Kaul (1978). It is

noted that when the natural frequency of the SDOF system is infinite, i.e., the SDOF system is a rigid body, Eq. (11) should produce

$$\lim_{\omega_c \to \infty} \sigma^2(\omega_c, \xi_c) = \lim_{\omega_c \to \infty} \int_{-\infty}^{+\infty} S_e(\omega) \left|H(\omega_c, \xi_c, \omega)\right|^2 d\omega = \sigma_g^2 = \int_{-\infty}^{+\infty} S_e(\omega) d\omega \tag{14}$$

where σ_g^2 is the variance of the ground acceleration. However, one can prove that the following integral based on the results from Eq. (13) is actually infinite and is not equal to σ_g^2.

$$\int_{-\infty}^{+\infty} S_e(\omega_c) d\omega_c = \int_{-\infty}^{+\infty} \frac{2\xi_c}{\pi|\omega_c|(1+4\xi_c^2)} \sigma^2(|\omega_c|, \xi_c) d\omega_c \neq \sigma_g^2 \tag{15}$$

The above result implies that the equivalent ground acceleration spectrum given by Eq. (13) cannot be applied to generate the ground motion when the SDOF is a rigid body. It is thus doubtable to use Eq. (13) as the equivalent acceleration spectrum. A new numerical method is proposed in this study to determine the equivalent ground acceleration spectrum.

3.2 Numerical method

The basic steps involved in the numerical method to find the equivalent ground acceleration excitation spectrum using Eq. (8) can be described as follows:

(1) Select the damping ratio φ_c and the natural frequency ϖ_c of the SDOF system and find the absolute acceleration response $R(\varpi_c, \varphi_c)$ of the SDOF system from the acceleration response spectrum given in a seismic design code. It is noted that most seismic design codes provide the acceleration response spectrum in the first principal direction within a certain range of natural frequency (period) only. When the natural frequency (period) is very small (large), the acceleration response can be assumed to be zero.

(2) Define the equivalent ground acceleration excitation spectrum $S_E(\varpi)$ in Eq. (8) within a certain range $[0\ \varpi_u]$, in which ϖ_u is the upper limit of integration and should cover the highest excitation frequency of interest. To be consistent with most of the existing ground acceleration excitation spectra, the ground acceleration excitation spectrum is set as zero at zero frequency in this study.

(3) Divide the range $[0\ \varpi_u]$ into n equal intervals $\Delta\varpi$ by means of points $0 = \varpi_0 < \varpi_1 < \varpi_2 < \cdots < \varpi_{n-1} < \varpi_n = \varpi_u$, in which $\Delta\varpi$ is equal to $\varpi_i - \varpi_{i-1}$ ($i = 1, 2, \cdots, n$). Within the ith interval $[\varpi_i - \varpi_{i-1}]$, $S_E(\varpi)$ is assumed to vary linearly from $S_E(\varpi_{i-1})$ to $S_E(\varpi_i)$, and so does the module value of the absolute acceleration response transfer function $\left|H(\omega_c, \xi_c, \omega)\right|^2$ in Eq. (8). As a result, the integral of $S_E(\varpi)\left|H(\omega_c, \xi_c, \omega)\right|^2$ on $[0\ \varpi_u]$ is given by

$$\int_0^{\omega_u} S_E(\omega) \left|H(\omega_c, \xi_c, \omega)\right|^2 d\omega =$$

$$\frac{\Delta\omega}{6}\left([2|H_0|^2 + |H_1|^2] S_E(\omega_0) + \sum_{i=1}^{n-1} [|H_{i-1}|^2 + 4|H_i|^2 + |H_{i+1}|^2] S_E(\omega_i) + [|H_{n-1}|^2 + 2|H_n|^2] S_E(\omega_n) \right) \tag{16}$$

in which $\left|H_i\right|^2$ denotes the value of $\left|H(\omega_c, \xi_c, \omega)\right|^2$ $(i = 0, 1, 2, \ldots, n)$.

(4) Considering a series of natural frequencies of the SDOF system $\varpi_c = \varpi_0, \varpi_1, \ldots, \varpi_n$ but with the same damping ratio φ_c (φ_c will be ignored in the following expression), Eqs. (8) and (16) lead to the following $n + 1$ equations

$$\begin{bmatrix} 2|H_{0,0}|^2+|H_{0,1}|^2 & \cdots & |H_{0,i-1}|^2+4|H_{0,i}|^2+|H_{0,i+1}|^2 & \cdots & |H_{0,n-1}|^2+2|H_{0,n}|^2 \\ \cdots & \cdots & \cdots & \cdots & \cdots \\ 2|H_{i,0}|^2+|H_{i,1}|^2 & \cdots & |H_{i,i-1}|^2+4|H_{i,i}|^2+|H_{i,i+1}|^2 & \cdots & |H_{i,n-1}|^2+2|H_{i,n}|^2 \\ \cdots & \cdots & \cdots & \cdots & \cdots \\ 2|H_{n,0}|^2+|H_{n,1}|^2 & \cdots & |H_{n,i-1}|^2+4|H_{n,i}|^2+|H_{n,i+1}|^2 & \cdots & |H_{n,n-1}|^2+2|H_{n,n}|^2 \end{bmatrix} \begin{bmatrix} S_E(\omega_0) \\ \cdots \\ S_E(\omega_i) \\ \cdots \\ S_E(\omega_n) \end{bmatrix} = \frac{6}{\Delta\omega} \begin{bmatrix} \left(\frac{R(\omega_0)}{r_p(\omega_0)}\right)^2 \\ \cdots \\ \left(\frac{R(\omega_i)}{r_p(\omega_i)}\right)^2 \\ \cdots \\ \left(\frac{R(\omega_n)}{r_p(\omega_n)}\right)^2 \end{bmatrix} \tag{17}$$

in which $|H_{i,j}|^2$ denotes the value of $|H(\omega_c, \omega)|^2$ when ω_c is equal to ω_i and ω is equal to ω_j (i, j = 0, 1, 2, …, n); $R(\omega_i)$ and $r_p(\omega_i)$ are, respectively, the response spectrum value and the peak factor at the natural frequency ω_i. It is noted in step 2 that $S_E(\omega_0)$ and $R(\omega_o)$ are set as zero and thus the first column and the first low in Eq. (17) can be eliminated. The numerical solutions of Eq. (17) can be found using the successive over-relaxation (SOR) method (Golub and Van Loan 1996) as follows

$$S_E(\omega_i)^{(k+1)} = \frac{r}{a_{ii}}\left(b_i - \sum_{j=1}^{i-1} a_{ij} S_E(\omega_i)^{(k+1)} - \sum_{j=i+1}^{n} a_{ij} S_E(\omega_i)^{(k)}\right) + (1-r) S_E(\omega_i)^{(k)}, \ (i = 1, \ldots, n) \tag{18}$$

in which

$$a_{ii} = |H_{i,i-1}|^2 + 4|H_{i,i}|^2 + |H_{i,i+1}|^2, \ a_{ij} = |H_{i,j-1}|^2 + 4|H_{i,j}|^2 + |H_{i,j+1}|^2, \ (i = 1, \ldots, n, \ j = 1, \ldots, n)$$

$$b_i = \frac{6}{\Delta\omega}\left(\frac{R(\omega_i)}{r_p(\omega_i)}\right)^2 \tag{19}$$

r is the relaxation parameter which is utilized to accelerate the solutions convergence, and it is taken as unit in this study. When using the iteration method expressed by Eq. (18) to find the numerical solution, the initial value for the equivalent ground acceleration excitation spectrum can be set as zero.

In the current practice, the three principal ground accelerations are often assumed to have identical spectral shape (Yamazaki and Ansary 1997, Menum and Der Kiureghian 1998). Therefore, once the equivalent ground acceleration excitation spectrum in the first principal direction is determined, the equivalent ground acceleration excitation spectrum in the second principal direction and the vertical direction can be determined by the proportionality rule. This study refers to the Chinese Code for Seismic Design of Buildings (GB50011 2001), the ratio between the second principal ground acceleration excitation spectrum and the first principal ground acceleration excitation spectrum is 0.73, and the ratio between the vertical ground acceleration excitation spectrum and the first principal ground acceleration excitation spectrum is 0.4.

4. Ground acceleration time history generation

Since the ground acceleration time histories will be generated for a high-tech facility along the structural axes rather than the principal directions, the most unfavorable ground acceleration excitation spectral matrix with respect to the structural axes can be determined using Eq. (1) based

on the ground acceleration excitation spectral matrix with respect to the principal directions and the critical angle as follows

$$\mathbf{S} = \begin{bmatrix} S_{xx} & S_{xy} & 0 \\ S_{yx} & S_{yy} & 0 \\ 0 & 0 & S_{zz} \end{bmatrix} = \mathbf{R} \begin{bmatrix} S_{11} & 0 & 0 \\ 0 & S_{22} & 0 \\ 0 & 0 & S_{33} \end{bmatrix} \mathbf{R}^T = \begin{bmatrix} \cos^2\theta S_{11} + \sin^2\theta S_{22} & \sin\theta\cos\theta(S_{11} - S_{22}) & 0 \\ \sin\theta\cos\theta(S_{11} - S_{22}) & \sin^2\theta S_{11} + \cos^2\theta S_{22} & 0 \\ 0 & 0 & S_{33} \end{bmatrix}$$
$$= \begin{bmatrix} (\cos^2\theta_c + \sin^2\theta_c k_2) S_{11} & \sin\theta_c\cos\theta_c(1 - k_2) S_{11} & 0 \\ \sin\theta_c\cos\theta_c(1 - k_2) S_{11} & (\sin^2\theta_c + \cos^2\theta_c k_2) S_{11} & 0 \\ 0 & 0 & k_3 S_{11} \end{bmatrix} \tag{20}$$

in which S_{ii} (i = 1, 2, 3) is the ith principal ground acceleration excitation spectrum; S_{xx}, S_{yy}, and S_{zz} are the ground acceleration excitation spectrum along the x-structural axis, y-structural axis, and z-structural axis, respectively; θ_c is the critical angle determined by Eq. (6) that renders the maximum response of the structure; k_2 is the ratio between the second principal excitation spectrum and the first principal excitation spectrum; k_3 is the ratio between the vertical excitation spectrum and the first principal excitation spectrum; and $S_{xy} = S_{yx}$ is the cross ground acceleration excitation spectrum in the horizontal plane between the x-structural axis and y-structural axis. From Eq. (20), one can see that if θ_c is equal to zero, $S_{xy} = S_{yx} = 0$; $S_{xx} = S_{11}$; $S_{yy} = S_{22}$; and $S_{zz} = S_{33}$. If θ_c is equal to $\pi/4$ or $3\pi/4$, the two horizontal ground acceleration excitations in the x-structural axis and y-structural axis are well correlated.

The most unfavorable ground acceleration time histories with respect to the structural axes can then be generated using the spectral representation method proposed by Deodatis (1996) based on the most unfavorable ground acceleration spectral matrix given by Eq. (20).

$$a_j(t) = \sqrt{2\Delta\omega} \sum_{m=1}^{j} \sum_{l=1}^{N} |H_{jm}(\omega_{ml})| \cos(\omega_{ml} t - \theta_{jm}(\omega_{ml}) + \phi_{ml}) \quad (j = x, y, z) \tag{21}$$

where $a_j(t)$ is the ground acceleration time history along the structural axis j ($j = x, y, z$); $\Delta\varpi$ is the frequency interval between the spectral lines which can be determined by ϖ_u/N; N is the total number of the frequency interval. $H_{jm}(\omega_{ml})$ is the (j, m) element of the low-triangle matrix $\mathbf{H}(\omega_{ml})$, given by

$$\mathbf{S}(\omega_{ml}) = \mathbf{H}(\omega_{ml})[\mathbf{H}^*(\omega_{ml})]^T \tag{22}$$

in which $\mathbf{S}$ is the most unfavorable ground acceleration excitation spectral matrix with respect to the structural axes given by Eq. (20); the superscript * signifies a complex conjugate; and the superscript T means the transpose operation of a matrix. Furthermore

$$\omega_{ml} = (l - 1)\Delta\omega + \frac{m}{j}\Delta\omega \tag{23}$$

$$\theta_{jm}(\omega_{ml}) = \tan^{-1}\left(\frac{\mathrm{Im}(H_{jm}(\omega_{ml}))}{\mathrm{Re}(H_{jm}(\omega_{ml}))}\right), \quad (j \geq m) \tag{24}$$

ϕ_{ml} is a random variable uniformly distributed between 0 and 2π. The ground acceleration time histories generated by Eq. (21) are stationary in theory. To account for the non-stationary characteristic of seismic ground acceleration, the most unfavorable stationary ground acceleration time histories obtained above are multiplied by an envelope function $M(t)$ to obtain the most unfavorable non-stationary ground acceleration time histories.

$$A_j(t) = M(t)a_j(t), \quad (j = x, y, z) \tag{25}$$

Jangid (2004) enumerated a few envelope functions for constructing the non-stationary ground motion time histories, in which the following segmentation equations are often used as the envelope function.

$$M(t) = \begin{cases} \left(\frac{t}{t_1}\right)^2, & (0 \le t \le t_1) \\ 1, & (t_1 \le t \le t_2) \\ \exp[-c(t-t_2)], & (t \ge t_2) \end{cases} \tag{26}$$

in which c is the constant. In accordance with the energy criteria, the parameters t_1 and t_2 can be determined by solving the following equation.

$$\frac{\int_0^{t_1}\left(\frac{t}{t_1}\right)^4 dt}{\int_0^{\infty} M^2(t)dt} = 0.05, \qquad \frac{\int_{t_1}^{t_2} dt}{\int_0^{\infty} M^2(t)dt} = 0.9 \tag{27}$$

If the value of c is taken as 0.85 s^{-1}, the parameters t_1 and t_2 can be obtained approximately as 2.5s and 13.6s, respectively. It is noted that the maximum value of the envelope function is unit over the whole time interval $[t_1, t_2]$ and its corresponding stationary time histories in $A_j(t)(j = x, y, z)$ are always compatible with the specified spectrum matrix aforementioned. Moreover, the most unfavorable peak ground acceleration obtained by Eq. (21) often remains in the most unfavorable non-stationary ground acceleration time history generated by Eqs. (25) and (26).

5. Case study

This case study considers a three-story reinforced-concrete high-tech building (facility) located at a seismic region of intensity 7 as specified in the Chinese Code for Seismic Design of Buildings (GB50011, 2001). The Chinese Code enforces the seismic design of building structures at three levels: no damage under the frequency earthquake with a probability of exceedance of 63% within 50 years; repairable under the design based earthquake with a probability of exceedance of 10% within 50 years; and no collapse under the maximum considered earthquake with a probability of exceedance of 2% within 50 years. Because the high-tech facility is extremely expense and it requires no damage during seismic event, the earthquake intensity is thus increased to 8 rather than 7 for its seismic design and only linear structural analysis is performed. In this regard, the acceleration response spectrum specified in the design code is first used to produce the equivalent

ground acceleration excitation spectrum in terms of the numerical method proposed in this study. The critical angle that renders the maximal response of the high-tech building is then determined using the response spectrum method as summarized in Section 2. The most unfavorable non-stationary ground acceleration time histories are finally generated and used to compute the seismic response of the high-tech building. All the computer programs for performing the aforementioned tasks are written using MATLAB as a platform.

5.1 Equivalent ground acceleration excitation spectrum

The site condition of the high-tech building is classified as Category 3 with a characteristic period of 0.45s. The corresponding acceleration response spectrum is given in Fig. 2 according to the Chinese Code for Seismic Design of Buildings (GB50011 2001) for a structural damping ratio of 0.05. It can be seen that the peak ground acceleration is about 1.06 m/s^2 at the period of zero. Within the range of period from 0.1s to 0.45s, the acceleration response value is constant of 2.35 m/s^2. As the period further increases from 0.45s, the acceleration response value decreases gradually to about 0.4 m/s^2 at the period of 6s. No further acceleration response value is provided by the design code after 6s. After taking into consideration the acceleration response spectrum given in Fig. 2 and the related natural frequencies of the building, the frequency range of the equivalent ground acceleration excitation spectrum in the first principal direction is decided from 0.2 Hz to 50 Hz with an interval of 0.2 Hz. As a result, the coefficient matrix in Eq. (17) has a dimension of 250. The coefficient matrix is computed and shown in Fig. 3, from which one can see that the diagonal elements are predominant. The equivalent ground acceleration excitation spectrum obtained by the proposed numerical method is displayed in Fig. 4. It can be seen that the dominant frequency corresponding to the peak acceleration is about 2.2 Hz, which coincides with the characteristic period of the site. To verify the accuracy of the equivalent ground acceleration excitation spectrum obtained by the numerical method, the excitation spectrum obtained is put into Eq. (8) to calculate the peak acceleration response spectrum. The calculated peak acceleration response spectrum is plotted in Fig. 2 to compare with the targeted one given by the design code. The relative

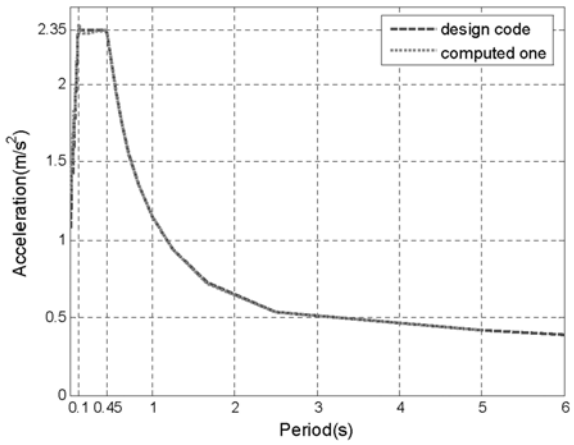

Fig. 2 Acceleration response spectrum (GB50011, 2001)

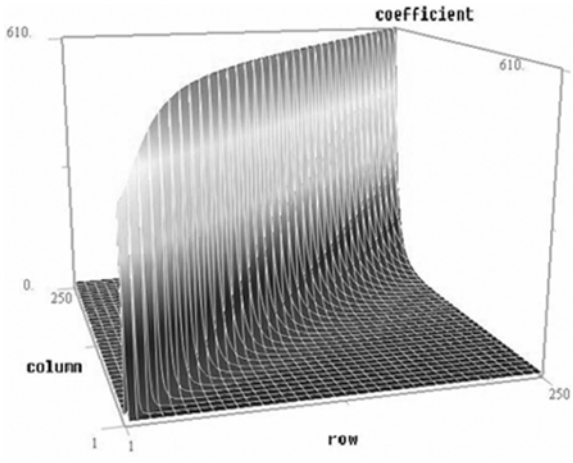

Fig. 3 Coefficient matrix in Eq. (17)

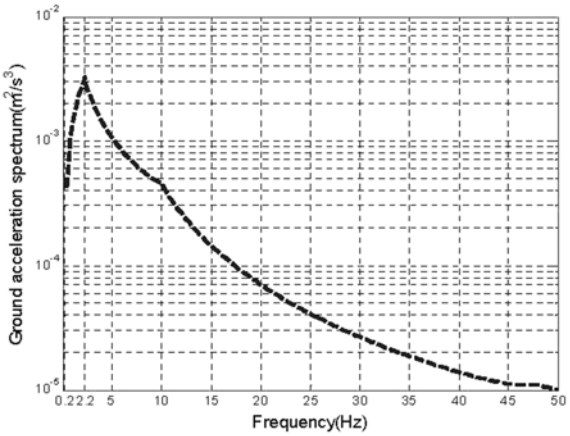

Fig. 4 Equivalent ground acceleration excitation spectrum

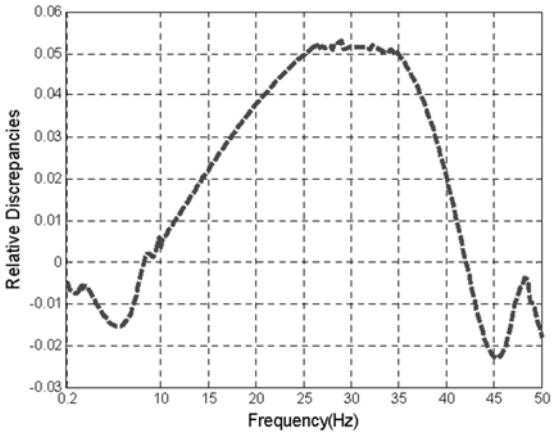

Fig. 5 Relative discrepancies between calculated and targeted response spectra

discrepancies between the two response spectra, that is, the differences between the calculated one and the targeted one divided by the targeted one, are shown in Fig. 5. It can be seen that at the low frequency range, the relative discrepancies are less than 3% and within the whole frequency range interested, the relative discrepancies are not more than 5%.

In accordance with the Chinese Code for Seismic Design of Buildings (GB50011 2001), all the three principal ground acceleration excitation spectra have the same shape. The ratio between the second principal ground acceleration excitation spectrum and the first principal ground acceleration excitation spectrum is 0.73, and the ratio between the vertical ground acceleration excitation spectrum and the first principal ground acceleration excitation spectrum is 0.4, by which all the three principal ground acceleration excitation spectra can be determined.

5.2 Finite element modeling and modal analysis

For the three-story high-tech building considered, its first and second stories are used as a double-level subfab and its third story is used as a clear room. The clear room sits on the second floor supported by a series of columns that provide both the horizontal and vertical stiffness to the second floor. A vast quantity of high-tech equipment is installed on the second floor. A long truss spans over the clear room to form the building roof and to support mechanical equipment such as cranes for installation and maintenance. The horizontal stiffness of the columns supporting the truss is much smaller than that supporting the second floor. A finite element model with a consistent mass matrix is established for the high-tech building, as shown in Fig. 6, in which all the beams and columns are modeled by 6DOF beam elements while the floors are modeled by 24DOF shell elements, resulting in a total of 439 nodes and a total of 2634 degrees of freedoms. The dimensions of the finite element model in plane and elevation are given in Fig. 7. The density and the modulus of elasticity of the concrete beam and column are taken as 2700 kg/m^3 and 3×10^{10} Pa, respectively. The average density of the first floor is 3845 kg/m^2 including the mass of equipment. The average thickness of the first floors is 0.25 m. Since the equipment is not arranged symmetrically with respect to the structure on the second floor, the average density of one part of the second floor is

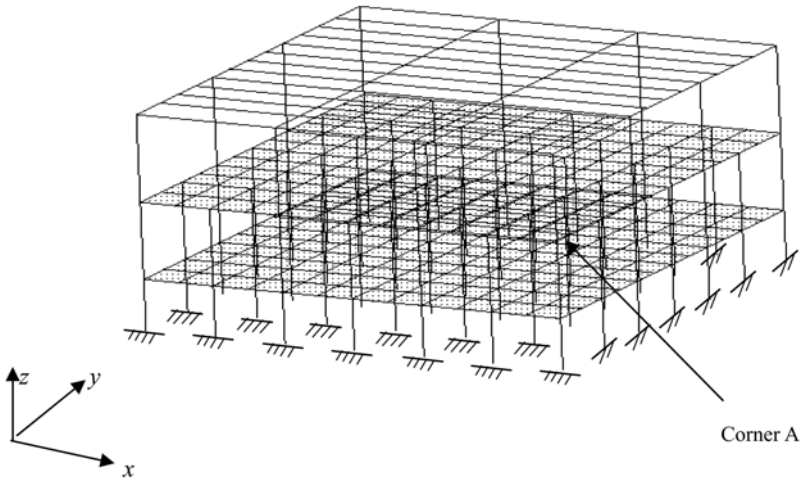

Fig. 6 Finite element model of the high-tech building

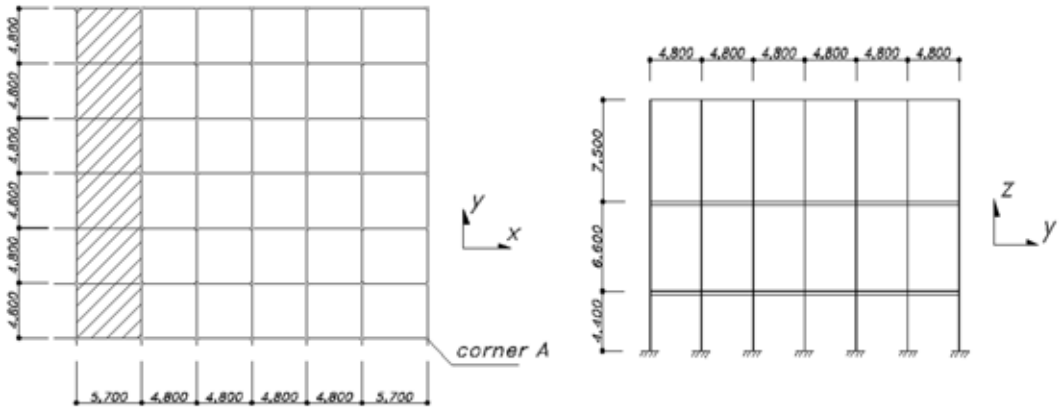

Fig. 7 Plane and elevation dimension (unit:mm)

about 3620 kg/m^2 including the mass of equipment while the average density of the other part (see shaded area in Fig. 7(a)) of the second floor is about 4000 kg/m^2 including the mass of equipment, leading to a small eccentricity about 0.18 m between the mass center and the stiffness center in the x-direction. The average thickness of the second floor is also 0.25 m. The cross-sectional properties of the beams in the first and second floor are identical. The beams are of rectangular cross section of 0.5 m × 0.7 m. The inner columns are of square cross section of 0.6 m × 0.6 m while the peripheral columns are of either L-, T- or rectangular cross section with the cross-sectional area ranging from 4.2 m^2 to 4.8 m^2.

After the finite element model is established, a modal analysis is carried out. The first 90 natural frequencies of the building are plotted in Fig. 8. They range from 1.98 Hz to 22.3 Hz. The first natural frequency of 1.98 Hz corresponds to the first lateral mode shape in the y-direction, as shown in Fig. 9(a), in which the solid line represents the mode shape. In the x-direction, the first natural frequency is 4 Hz and the corresponding mode shape is shown in Fig. 9(b).

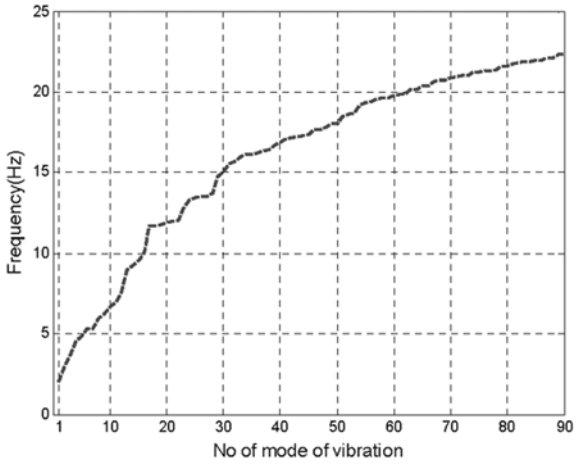

Fig. 8 The first 90 natural frequencies

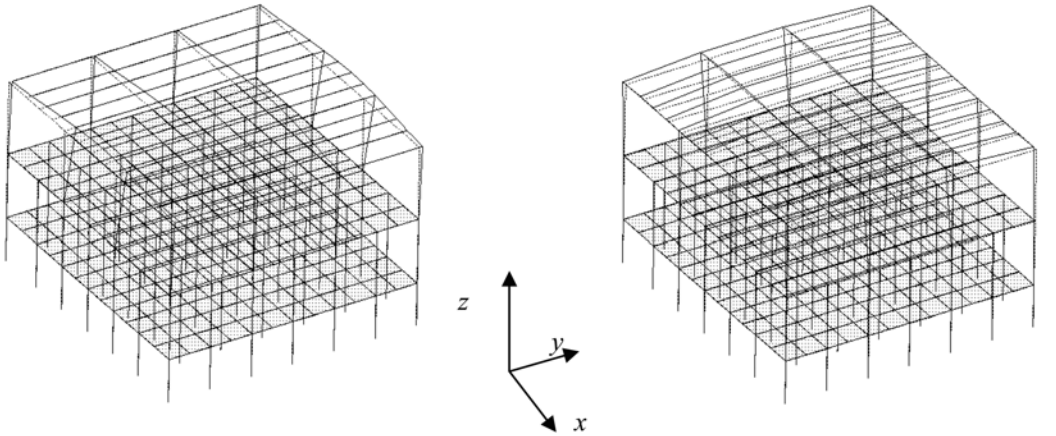

(a) The first mode in *y*-direction (b) The first mode in *x*-direction

Fig. 9 Selected mode shapes

5.3 Maximum structural responses at critical angles

For the high-tech building subject to seismic ground motion, the inter-story drift should be examined for the safety of the building and the acceleration response should be checked for the safety of high-tech equipment. Accordingly, the critical angles about both the acceleration response and the inter-storey drift should be determined using the response spectrum method introduced in Section 2. Since the clean room is located on the second floor, the acceleration responses of the second floor at the building geometric center and at the building corner A (see Fig. 6) are examined in this study and selected to determine the critical angles. The inter-story drifts between the second floor and the building roof at the building center and the building corner A are also examined and selected to determine the critical angles because the horizontal stiffness of the top story is quite small and the largest inter-story drift is expected to occur in the top story.

Eqs. (2) to (5) can be used to determine the variation of the structural response with angle θ and

to compute the maximum structural response using the acceleration response spectra specified in the Chinese Code for Seismic Design of Buildings (see Fig. 2). In the computation, the first and second modal damping ratios of the building are assumed to be 0.05. The higher modal damping ratios are determined based on the Rayleigh damping assumption and are then modified according the design code. A total of 90 modes of vibration are taken into account in the response computation. Figs. 10(a) and (b) show the variations of the peak acceleration response of the second floor at the building center in the x-direction and the y-direction, respectively, with angle θ. The maximum acceleration response in the y-direction is about 1.90 m/s^2 while the maximum acceleration response in the x-direction is about 1.52 m/s^2. The critical angle is almost 90^o corresponding to the maximum acceleration response in the y-direction. This critical angle is the same as that calculated using Eq. (6). The variations of the peak acceleration response of the second floor at the building corner in the x-direction and the y-direction with angle θ are depicted in Figs. 11(a) and (b) respectively. The

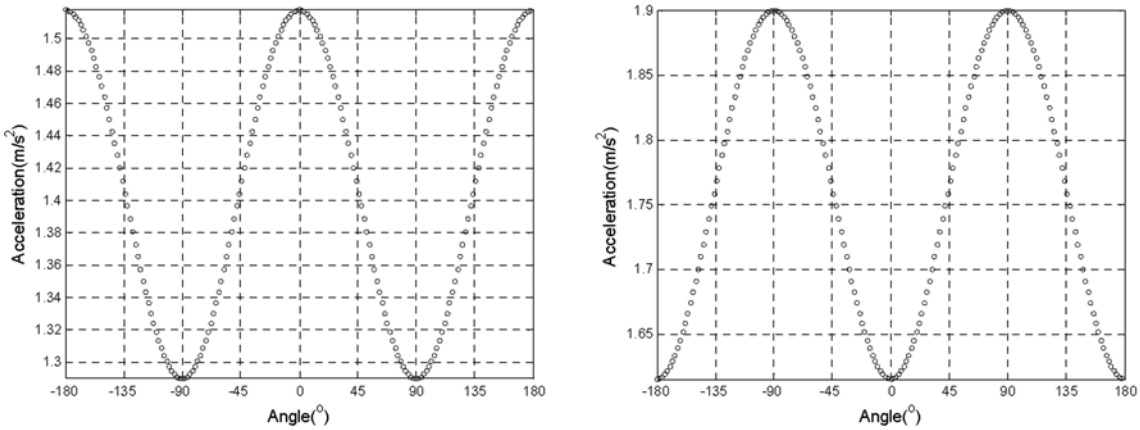

Fig. 10 Variations of acceleration responses with angle θ (second floor center)

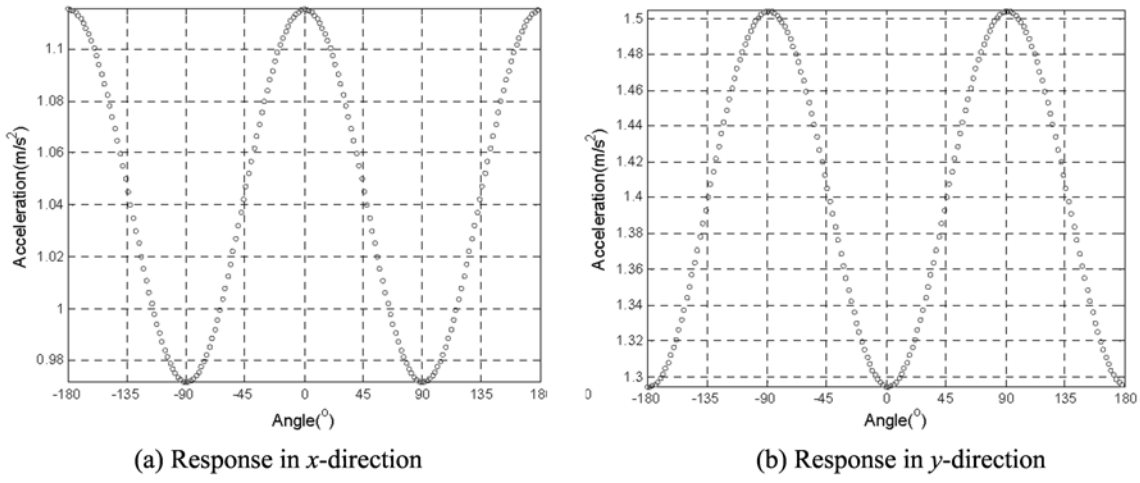

Fig. 11 Variations of acceleration responses with angle θ (second floor corner)

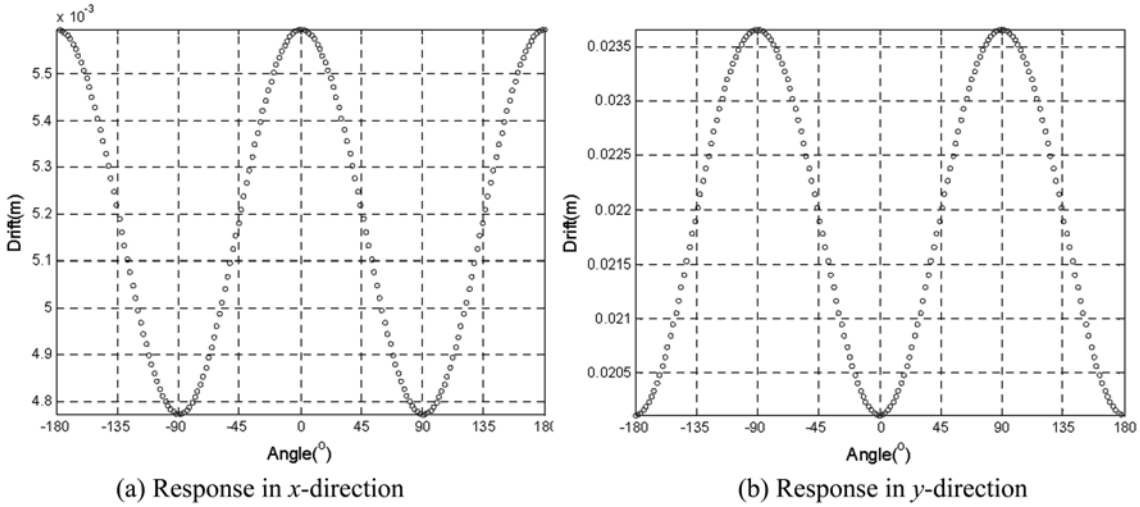

Fig. 12 Variations of Inter-storey drifts with angle θ (top story center)

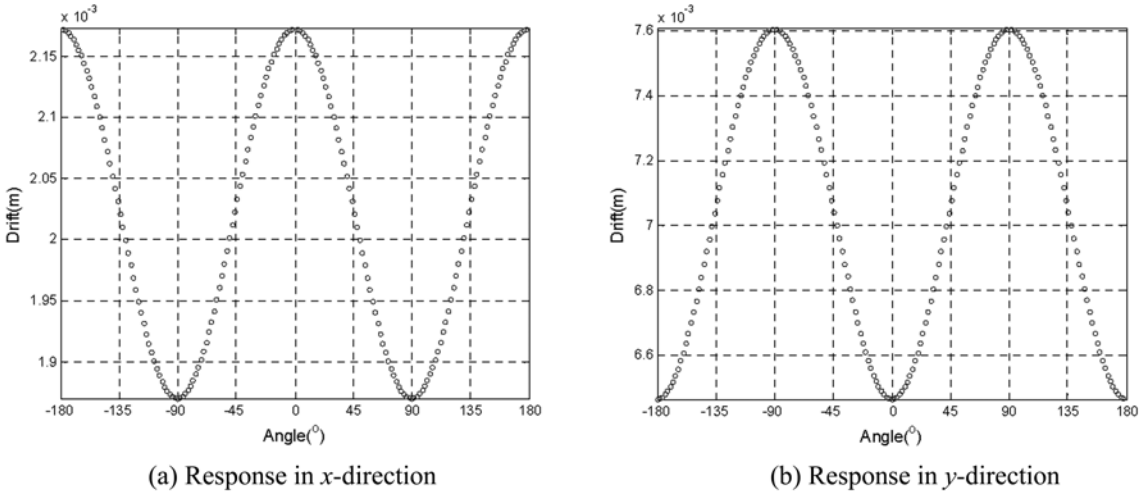

Fig. 13 Variations of inter-storey drifts with angle θ (top story corner)

maximum acceleration response in the y-direction is slightly more than 1.50 m/s^2 while the maximum acceleration response in the x-direction is slightly more than 1.1 m/s^2. As the columns uniformly located at the peripheral locations of the building take the large dimensions, resulting in the large torsional stiffness of the building section, the torsional effects due to the small eccentricity between the mass center and the stiffness center are very insignificant so as not to be detected.

For the inter-story drift between the second floor and the building roof (called the top story drift) at the building center, its variation with angle θ is shown in Fig. 12. The maximum drift in the y-direction is about 23.6 mm while the maximum drift in the x-direction is about 5.6 mm. The critical angle is almost 90^o corresponding to the maximum drift in the y-direction. This critical angle is also the same as that calculated using Eq. (6). The variations of the top story drift at the building corner

in the x-direction and the y-direction with angle are depicted in Figs. 13(a) and (b), respectively. The maximum drift in the y-direction is 7.60 mm while the maximum drift in the x-direction is 2.17 mm. The critical angle is also almost 90^{o} for the maximum drift in the y-direction because there is no eccentricity in the building roof.

5.4 Most unfavorable ground acceleration time histories

From the numerical results of the most unfavorable structural responses obtained above, one may conclude that the critical angle θ_c for the concerned high-tech building is 90^{o} corresponding to both the maximum acceleration response and the maximum top story drift. Eq. (20) can then be used to find the most unfavorable ground acceleration spectral matrix, and Eqs. (21)-(27) can be used to generate the most unfavorable ground acceleration time histories along the structural x- y- and z-axes. In the numerical simulation using Eq. (21), N is taken as 500 and $\Delta\varpi$ is taken as 0.628 rad/s. For the envelope function, the value of c is taken as 0.85 s^{-1} and the parameters t_1 and t_2 are obtained approximately as 2.5s and 13.6s, respectively. Displayed in Fig. 14 is the most unfavorable ground acceleration time histories generated for the concerned high-tech building, in which the peak ground acceleration is about 1.1 m/s^2 appearing in the y-direction.

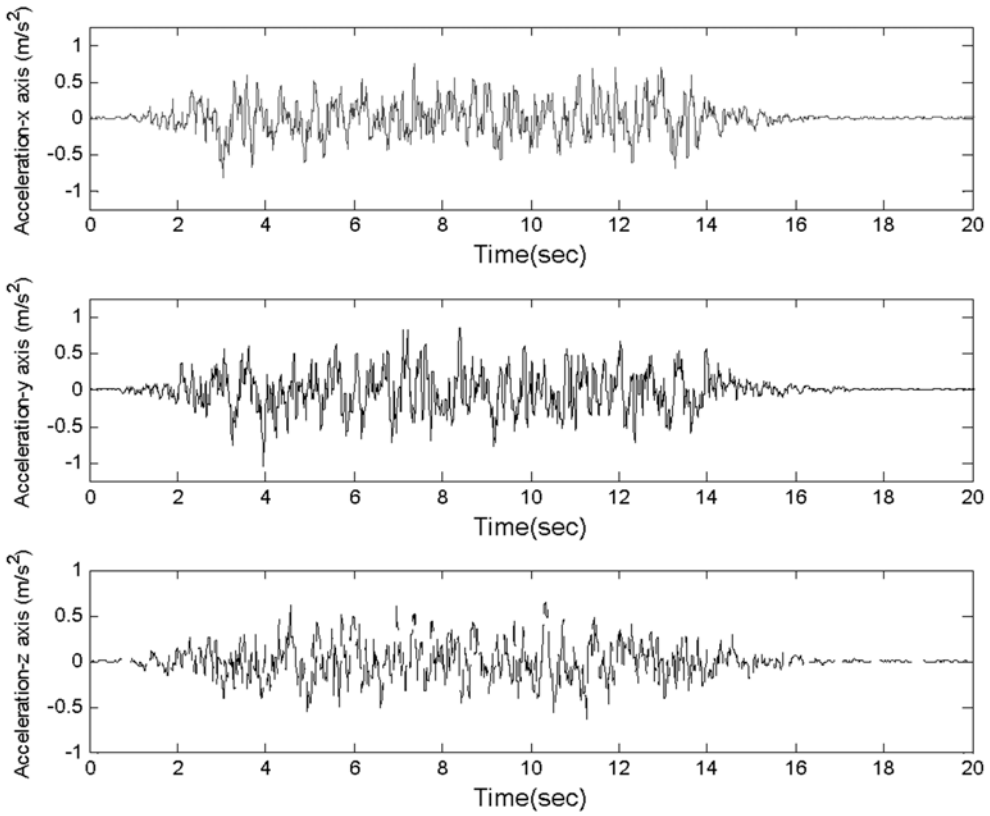

Fig. 14 Most unfavorable ground acceleration time histories

5.5 Comparison

With the most unfavorable ground acceleration time histories and the finite element model of the high-tech building, the structural response can be computed in the time domain and the maximum response can then be compared with those obtained from the response spectrum method. For the numerical computation of structural response in the time domain, the Newmark-β method is utilized and the Rayleigh damping assumption remains. Fig. (15) shows the acceleration response time histories of the second floor at the building center in the x-direction and the y-direction. The maximum acceleration response in the y-direction is about 2.05 m/s^2, and the maximum acceleration response in the x-direction is about 1.35 m/s^2. The maximum peak acceleration response in the y-direction obtained by the response spectrum method is approximately 1.90 m/s^2, as shown in

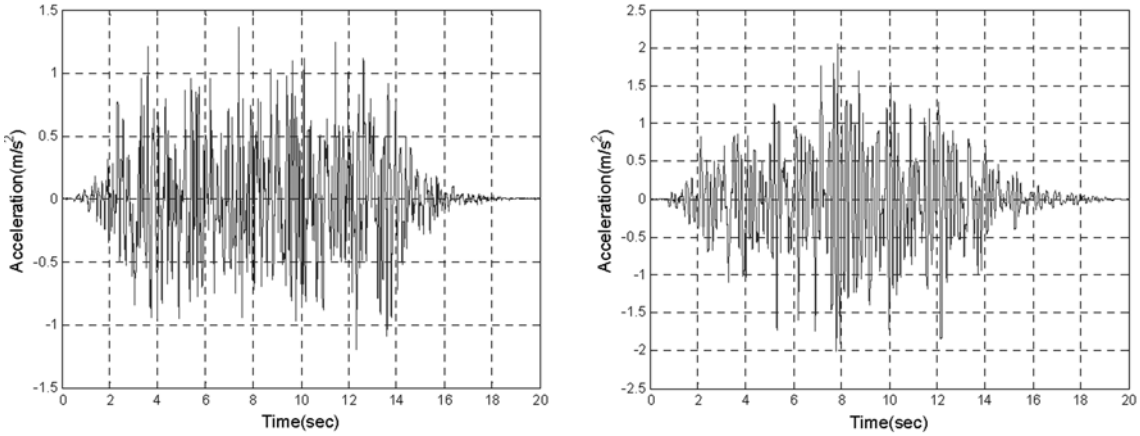

(a) Response in x-direction (b) Response in y-direction

Fig. 15 Time histories of acceleration response at the second floor center

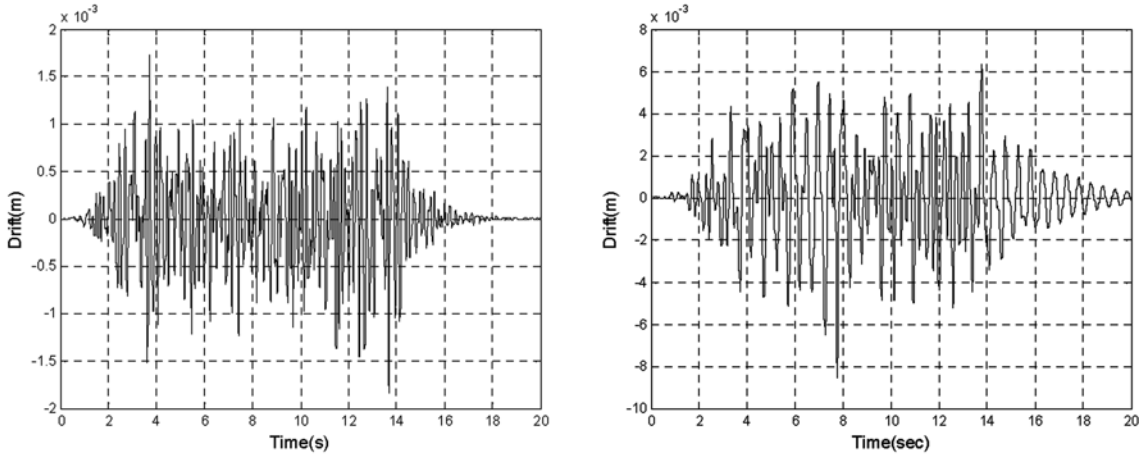

(a) Response in x-direction (b) Response in y-direction

Fig. 16 Time histories of top story drifts at the building corner

Fig. 10(b), which is close to 2.05 m/s^2. Fig. 10(b) also demonstrates that the first principle direction of earthquake coincides with the y-structural axis in this case study and the critical angle is therefore almost $\pm 90^o$. At the critical angle of $\pm 90^o$, the x-directional peak acceleration response obtained by the response spectrum method is about 1.28 m/s^2 as shown in Fig. 10(a), which is very close to 1.35 m/s^2 computed in the time domain and shown in Fig. 15(a). Displayed in Fig. (16) are the top-story drift time histories at the building corner in the x-direction and the y-direction. The maximum top story drifts in the y-direction are 8.30 mm which is close to the 7.60 mm obtained by the response spectrum method and shown in Fig. 13(b). The x-directional peak drift response obtained in the time domain and shown in Fig. 16(a) is about 1.75 mm which is also close to 1.87 mm obtained by the response spectrum method and shown in Fig. 13(a) at the angle either 90^o or -90^o. The comparative results demonstrate the feasibility of the proposed approach.

5.6 Further discussion

The type of structural system and the number of stories of the reinforced-concrete high-tech building discussed above are common in high-tech industries. The major possible reason which may cause torsional irregularity is the mass distribution of heavy high-tech equipment over the building floor. Therefore, the torsional rigidity of the high-tech building is normally designed to be large against torsional vibration. Nevertheless, to demonstrate the feasibility of the proposed strategy for a building with different torsional irregularities and structural systems, the mass distribution of equipment over the second floor in the previous case is changed. All the mass of the equipment is now concentrated on the shaded area shown in Fig. 7(a) of the second floor, which results in the average density of 16000 kg/m^3 over that area. The average density of the other part of the second floor is about 2500 kg/m^3 only. This arrangement leads to the eccentricity of 4.2 m between the mass center and the stiffness center in the x-direction. Furthermore, the peripheral columns between the first floor and second floor are removed to reduce torsional rigidity of the second story to form a suppositional building.

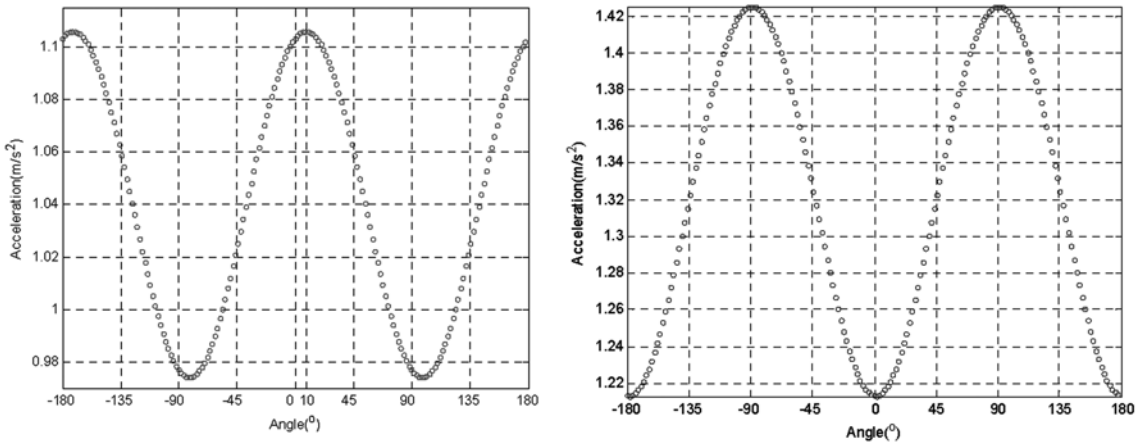

(a) Response in x-direction (b) Response in y-direction

Fig. 17 Variations of acceleration responses with angle θ (second floor corner A of suppositional building)

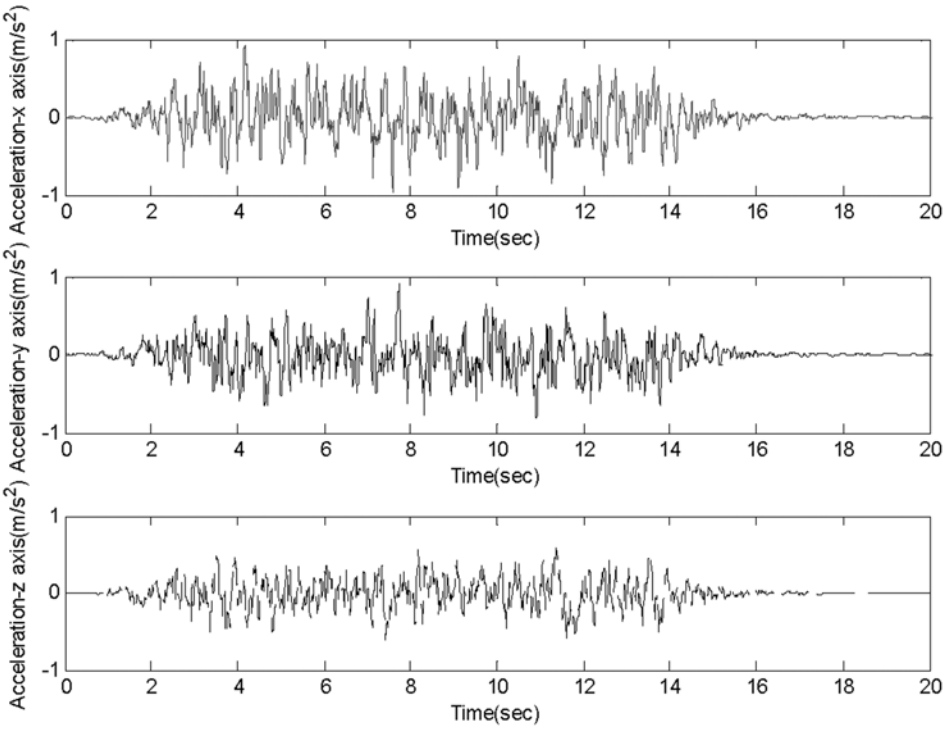

Fig. 18 Most unfavorable ground acceleration time histories for suppositional building

The critical angle about the acceleration response of the suppositional building at corner A is subsequently explored by using the same procedure as used in section 5.3. Fig. 17(a) and (b) plot the variations of the peak acceleration response of the second floor at the building corner A in the x-direction and the y-direction, respectively, with angle θ. It can be seen that the maximum acceleration response in the x-direction is about 1.11 m/s^2, which corresponds to a critical angle 10^o. The maximum acceleration response in the y-direction is about 1.43 m/s^2 with a critical angle slightly from 90^o by 1^o. The difference of critical angle between the x-direction and the y-direction is because of the torsional irregularity and the ratio of two seismic components in the two principle directions. To demonstrate the feasibility of the proposed strategy for the current building, Eq. (20) is then used to find the most unfavorable ground acceleration spectral matrix, and Eqs. (21)-(27) are used to generate the most unfavorable ground acceleration time histories for the maximum acceleration response of the building corner A in the x-direction with the critical angle θ_c of 10^o. The generated ground acceleration time histories are plotted in Fig. 18, in which the maximum ground acceleration is about 0.98 m/s^2 in the x-direction.

By applying the generated ground acceleration time histories to the suppositional building, the acceleration response of the building corner A can be computed in the time domain, and the maximum responses can then be compared with those obtained by the response spectrum method. Figs. 19(a) and (b) show the acceleration response time histories of the second floor at the building corner A in the x-direction and the y-direction, respectively. The maximum acceleration response in the x-direction is 1.18 m/s^2, which is close to 1.11 m/s^2 obtained by the response spectrum method and showed in Fig. 17(a). The maximum acceleration response in the y-direction is 1.33 m/s^2, which

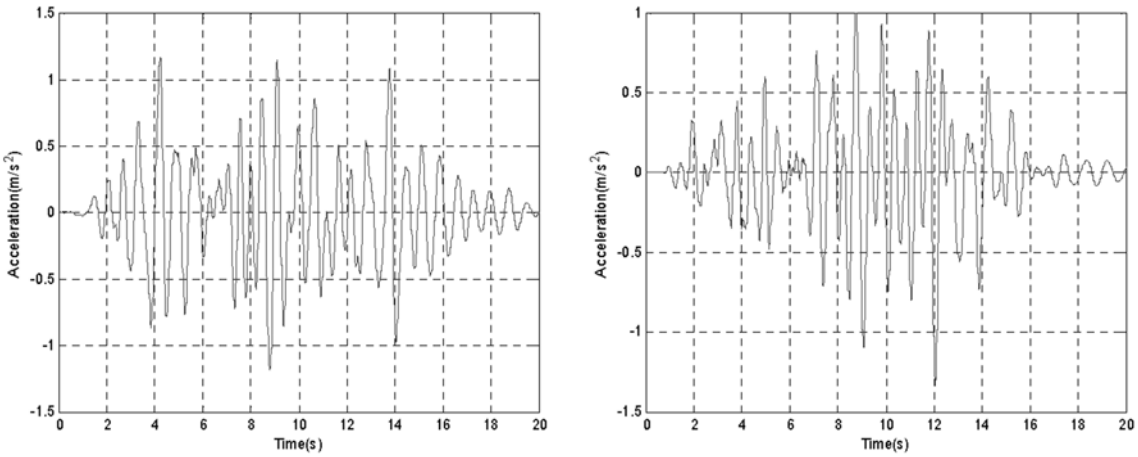

Fig. 19 Time histories of acceleration responses at the corner of suppositional building

is also close to 1.22 m/s^2 obtained by the response spectrum method. The value of 1.22 m/s^2 is obtained from Fig. 17(b) at the angle θ of 10^o. The comparative results demonstrate the feasibility of the proposed strategy for the building with different torsional irregularities and structural systems to some extent through this example.

6. Conclusions

The framework for generating three-dimensional critical seismic ground acceleration time histories compatible with the response spectra specified in design codes for high-tech facilities has been established in this study. This involves the identification of the most critical directions of seismic ground motions associated with the maximum response of a high-tech facility, the generation of the power spectrum density functions of ground accelerations compatible with the response spectra specified in design codes in critical directions, and the simulation of the most favorable non-stationary ground acceleration time histories along the structural axes. The proposed framework has been applied to a typical three-story reinforced-concrete high-tech building located in a seismic region referring to the Chinese Code for Seismic Design of Buildings (GB50011 2001). The three-dimensional critical seismic ground acceleration time histories generated according to the proposed framework have been used to compute both acceleration and inter-story drift time histories of the building. The computed maximum acceleration responses and inter-story drifts in the time domain have been compared with those obtained by the response spectrum method. The comparative results are satisfactory, demonstrating the feasibility and accuracy of the proposed approach.

Acknowledgements

The writers are grateful for the financial support from the Research Grants Council of Hong Kong through a CERG grant (PolyU 5054/02E).

References

Crempien-Laborie, J.E. and Orosco, L. (2000), "An evolutionary ground motion model for earthquake analysis of structures in zones with little history", *Soil Dyn. Earthq. Eng.*, **20**, 373-379.
Deodatis, G. (1996), "Simulation of ergodic multivariate stochastic processes", *J. Eng. Mech.*, **122**, 778-787.
GB50011 (2001), *Chinese Code for Seismic Design of Buildings*, Architectural Industry Publishing House, Beijing (in Chinese).
Golub, G.H. and Van Loan, C.F. (1996), *Matrix Computation*, Hopkins University Press House, Hopkins, Baltimore, USA.
Gupta, I.D. and Trifunac, M.D. (1998), "Defining equivalent stationary psdf to account for nonstationarity of earthquake ground motion", *Soil Dyn. Earthq. Eng.*, **17**, 89-99.
Jangrid, R.S. (2004), "Response of SDOF system to non-stationary earthquake excitation", *Earthq. Eng. Struct. Dyn.*, **33**, 1417-1428.
Joshi, A. and Midorikawa, S. (2004), "A simplified method for simulation of strong ground motion using finite rupture model of the earthquake source", *J. Seismol.*, **8**, 467-484.
Kaul, M.J. (1978), "Stochastic characterization of earthquakes through their response spectrum", *Soil Dyn. Earthq. Eng.*, **6**, 497-509.
Li, J.H. and Li, J. (2005), "A response spectrum method for seismic response analysis of structures under multi-support excitations", *Struct. Eng. Mech.*, **21**, 255-273.
Lopez, O.A. and Torres, R. (1997), "The critical angle of seismic incidence and the maximum structural response", *Earthq. Eng. Struct. Dyn.*, **26**, 881-894.
Menun, C. and Der Kiureghian, A. (1998), "A replacement for the 30%, 40%, and SRSS rules for multi-component seismic analysis", *Earthq. Spectra,* **14**, 153-156.
Olafsson, S., Remseth, S. and Sigbjornsson, R. (2001), "Stochastic models for simulation of strong ground motion in Iceland", *Earthq. Eng. Struct. Dyn.,* **30**, 305-1331.
Taskin, B. and Hasgür, Z. (2006), "Monte Carlo analysis of earthquake resistant R-C 3D shear wall-frame structures", *Struct. Eng. Mech.*, **22**, 371-399.
Yamazaki, F. and Ansary, M.A. (1997), "Horizontal-to-vertical spectrum ratio of earthquake ground motion for site characterization", *Earthq. Eng. Struct. Dyn.,* **26**, 671-689.